2019 2nd IEEE International Conference on Soft Robotics (RoboSoft)
COEX, Seoul, Korea, April 14-18, 2019

Simulation–based Design of Transfer Support Robot and Experimental Verification

Yumeko Imamura[1], Yui Endo[1] and Eiichi Yoshida[1]

Abstract— **The need for robotic care devices that support the movements of the elderly is increasing with demographic changes in modern societies. Such devices should be designed and controlled while considering their physical effects on users, since the devices make direct contact with the users and move their body. However, human physical burdens are difficult to evaluate for machines that undergo complex interactions with humans, and little research has focused on the care robots' effects on the human body. We have proposed a simulation–based optimization method of the design parameters, which uses a digital model of the human body. The user is represented as a link model, and the joint torques and contact forces on this model are analyzed. The motion trajectories of the device were then designed according to the simulation results. To verify this design method, we then performed an experiment with human subjects and measured the contact forces between human and device using a custom mockup of the transfer aid robot.**

Index Terms— **Soft Robot Applications, Physically Assistive Devices, Product Design, Physical Human-Robot Interaction, Digital human.**

I. INTRODUCTION

The demand for elder-care workers is increasing due to the rapidly aging population, and the burden on individual caretakers has been increasing [1]. Especially manually transferring and lifting work of a care receiver imposes a heavy burden on the caretakers. The use of mechanical aids has been encouraged to help caretakers perform their jobs more safely and effectively [2]. Such robotic care devices make direct contact with the care receivers to support their movements. The devices should be designed with consideration of physical effects on the care receivers, therefore, soft robotics technologies such as soft materials and deformable structures are desirable to be introduced. The contact surfaces of general care robots on the market are using soft materials in order to avoid unnecessary force concentration. However, it is difficult to evaluate quantitatively the load on human subjects when using machines that undergo complex interaction with the user. Few systematic studies have been published about the design and evaluation of care robots taking the effects on the user's body as a design index.

In the research field, assistive devices are often assessed with actual measurements such as surface electromyograms [3][4][5]. However, when evaluating the devices in subject experiments during the development phase, the actual machine often must be revised and measured with human subjects every time, leading to costly experimental procedures. Meanwhile, virtual simulations of the robot-human interactions could offer relevant quantitative data at a much lower cost.

Several commercial software packages are available for biomechanical simulation with digital human models [6]. For instance, JACK (Siemens AG) is a human modeling and simulation software for ergonomic assessment [7]. Anybody (AnyBody Technology A/S) is a software with greater emphasis on dynamic evaluation, and it can be used for ergonomics assessment as well as more-detailed biomechanical analysis such as the estimation of muscle activity [8]. However, in these ergonomic analyses, external forces still need to be estimated by the user, since the contact forces in case of multiple contacts cannot be uniquely determined.

As an example of modeling human motion and analyzing it in light of robotic assistance, Geravand et al. proposed a dynamic model of the sit-to-stand motion [9]. They adopt a simplified human model with one contact point on the device and demonstrated a method to generate assistance trajectories according to the user's physical weakness. This method is an effective tool for developing assistive devices. On the other hand, a method is needed that can treat multi-point contact for analyzing the other type of devices.

In this paper, we treat the transfer support robot *Hug* (Fuji Corp. [10]) as a target device. Hug is a device that assists an elderly care receiver to stand from the sitting posture. This robot is also intended to prevent patients from becoming bedridden by actively helping the patient to practice sitting and standing when his or her muscular power has declined. Thus, unlike lifts that transfer the users by keeping them in a seated or lying posture, this device guides the user to a stoop–standing posture. The user can reduce the load on the joint torques by leaning the body to the device. However, if the force supporting the body concentrates on a certain part, it becomes uncomfortable for the user. It is desirable

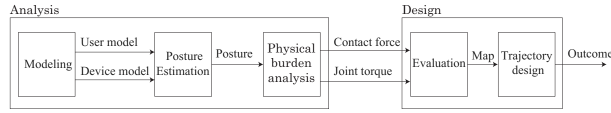

Fig. 1. Outline of evaluation framework.

[1]Y. Imamura, Y. Endo and E. Yoshida are with CNRS-AIST Joint Robotics Laboratory, UMI3218/RL, Intelligent Systems Research Institute, National Institute of Advanced Industrial Science and Technology, 1-1-1 Umezono, Tsukuba, Ibaraki 305-8560 Japan. {yumeko.imamura, y.endo, e.yoshida}@aist.go.jp

to develop the device while checking the distribution of the supporting forces.

We have been developing a simulation–based design method that optimizes the device parameters based on the analysis using a digital human model [11][12]. In the previous paper [13], we proposed a basic concept of the design framework. The proposed method represents the user as a link model and estimates the user's posture when using the assistive robot and analyzes the physical load on users. We then build a map of evaluation measures with respect to the design parameters to be optimized.

In this paper, we verify this design method with a human subject experiment. We developed a mockup of the assistive robot and measured the user's muscle activities and human–device contact forces. We also designed motion trajectory patterns of the device with the proposed method. The experiment results show that the proposed method can design device movement trajectories that place less burden on the selected body part. The rest of this paper is organized as follows. Section 2 outlines the proposed design method before describing an application example with a model of the mockup in Section 3. Section 4 describes the measurement experiments with human subjects and the verification results. Finally, Section 5 concludes the paper.

II. Simulation–based Design

In this chapter, we will describe our proposed method that evaluates and designs devices using analysis of the physical burden on the user. The evaluation and design flow is shown in Fig. 1. First, we explain the method of modeling and physical burden analysis, then propose the method of designing device based on the analysis result.

A. Analysis

1) Modeling: First, the device and human user are modeled using the virtual ergonomic assessment software *DhaibaWorks* [11], [12]. The software constructs whole–body human models based on a database of anthropometric dimensions; therefore, it can generate a model that has an individualized physique without actual measurements by estimating whole–body anthropometric dimensions from a sparse set of dimensions. The human model consists of a link model and skin–surface meshes. The link model consists of links connected by joints. As for mechanical properties, each link has mass, center of mass, inertia matrix. When the joint rotates, the neighboring skin surface mesh deforms according to the Skeletal Subspace Deformation algorithm [14]. The device is also modeled as a rigid–link system and can be associated with three–dimensional geometric meshes.

2) Posture estimation: To estimate the user's posture when using the device, the positional relationship between the user and the device is defined. Anatomical feature points are defined on the human skin surface mesh and the same number of feature points are defined on the device model. The joint angles of the human link model that minimize the distances between the corresponding feature points are calculated using an inverse kinematics algorithm. This allows us to ensure correspondence between the device and human postures. The algorithm can also estimate how the user posture changes in response to different motions or device dimensions.

3) Physical burden analysis: As for the physical load on the human, the joint torques exerted by the human and contact forces between the human and the device or environment are analyzed using the human body dynamics simulator [15]. The joint torques of the human link model $\boldsymbol{\tau}_0$ that achieve a given posture without contact forces, can be calculated using inverse dynamics computation.

$$\boldsymbol{\tau}_0 = \boldsymbol{M}(\boldsymbol{q})\ddot{\boldsymbol{q}} + \boldsymbol{c}(\boldsymbol{q}, \dot{\boldsymbol{q}}) + \boldsymbol{g}(\boldsymbol{q}) \tag{1}$$

where,

- $\boldsymbol{q}$ is the generalized coordinates that include the global position and posture of the link model and the angles of each joint,
- $\boldsymbol{M}$ is the inertia matrix,
- $\boldsymbol{c}$ is the Coriolis and centrifugal term,
- $\boldsymbol{g}$ is the gravity term.

Next, based on the calculated torques $\boldsymbol{\tau}_0$, the joint torques are recalculated while estimating the external forces. For the estimation of contact force, coulomb friction is assumed, and contact forces are approximated as a convex polyhedral cone (Fig. 2) defined by the normal vector of the contact and the friction coefficient μ [16]. If no slip occurs at the contact point, the contact force vector $\boldsymbol{F}_i$ is represented as the resultant force of the forces on each edge $\boldsymbol{e}_{i,j}$ of the polyhedral cone.

$$\boldsymbol{F}_i = \sum_{j=1}^{m} f_{i,j}\boldsymbol{e}_{i,j} \tag{2}$$

where m is the number of edges and $f_{i,j}$ is the magnitude of the force at each edge. The following vector is defined by collecting the coefficients for all contact points.

$$\boldsymbol{f} = [f_{1,1}\ f_{1,2}\ \dots\ f_{n,m}]^{\mathrm{T}} \tag{3}$$

where, n is the number of the contact points.

To estimate the joint torques and contact forces, we solve the following quadratic programming problem.

$$\begin{aligned} &\min : \|\boldsymbol{W}_f{}^{\frac{1}{2}}\boldsymbol{f}\|^2 + \|\boldsymbol{W}_\tau{}^{\frac{1}{2}}\left(\boldsymbol{\tau}_0 - \boldsymbol{J}^T\boldsymbol{f}\right)\|^2 \\ &\text{subject to} : \boldsymbol{f} \geq \boldsymbol{0} \end{aligned} \tag{4}$$

where $\boldsymbol{f}$ is the vector of parameters to be optimized and $\boldsymbol{J}^T$ is the matrix that converts $\boldsymbol{f}$ into joint torques. $\boldsymbol{W}_f$ and $\boldsymbol{W}_\tau$ are weighting matrices. Both are diagonal matrices and their elements are positive values w_f, w_b, w_j.

$$\boldsymbol{W}_f = w_f\boldsymbol{I}_{nm} \tag{5}$$

$$\boldsymbol{W}_\tau = \begin{bmatrix} w_b\boldsymbol{I}_6 & \boldsymbol{0} \\ \boldsymbol{0} & w_j\boldsymbol{I}_{(DOF-6)} \end{bmatrix} \tag{6}$$

where $\boldsymbol{I}$ is the identity matrix. The first term of Eq. 4 minimizes the contact forces, and the second term $\left(\boldsymbol{\tau}_0 - \boldsymbol{J}^T\boldsymbol{f}\right)$ is

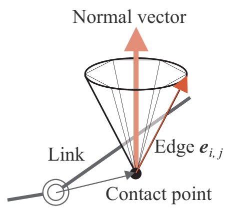

Fig. 2. Convex polyhedral cone approximation of contact forces.

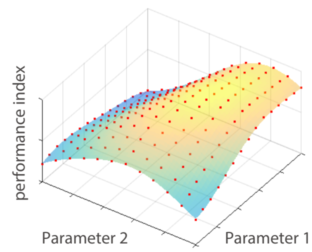

Fig. 3. Sample evaluation map. The horizontal axes are device parameters and the vertical axis is evaluation values. The red dots show discrete analysis results and the curved surface obtained by fitting the analysis results is used for parameter design.

the joint torque exerted by human when the estimated contact forces are applied. If w_f increases, the solution of the contact forces decreases, and if w_j is increased, the joint torque exerted by the human decreases. w_b is a weight on the forces acting on the base link that represents the global position and attitude of the link model. The base link is moved only by external forces such as the floor reaction force [17]. When the weight w_b is reduced, the errors between the external forces necessary for the input posture and the result become large. The details are discussed in a paper we published previously [13].

B. Design

1) Evaluation map: A map of physical burden is generated in preparation for design of the device. This evaluation map models the relationship between device parameters and evaluation values. Here velocity and acceleration are not taken into consideration and we assumed a one-to-one correspondence between the device parameters and physical burden, because the support robot typically moves at low speed for the sake of user safety.

When the number of the design parameters is N, a set of the design parameters $\boldsymbol{x} = [x_1\ x_2\ ...\ x_N]$ is defined. The designer generates combinations of values discretely cover the whole possible range of parameters. Posture estimation and burden analysis are performed for each parameter combination, yielding the evaluation values. Various factors such as the joint angle, joint torque and contact force can be used for this evaluation value. A threshold can also be set for those evaluation measures based on an ergonomic knowledge.

Then, evaluation values and the device parameters are normalized between 0 and 1, and the evaluation values are approximated with the expression $\hat{E}_k(\boldsymbol{a}_k, \boldsymbol{x})$ for interpolating discrete values. $\boldsymbol{a}_k$ is a coefficient vector. When multiple burden indexes are of interest, a comprehensive evaluation map can be created by combining values with arbitrary weights w_k.

$$E(\boldsymbol{a}, \boldsymbol{x}) = \sum_k w_k \hat{E}_k(\boldsymbol{a}_k, \boldsymbol{x}) \tag{7}$$

The weights w_k are determined by the designer according to the importance of each evaluation measure. If only two design parameters are relevant, the evaluation map can be drawn as in Fig. 3. The higher performance index on the vertical axis indicates the larger physical loads. Quantitative evaluation values can be obtained for arbitrary design parameters using this map.

2) Trajectory design: Finally, the trajectory design using the evaluation map is shown as an example of application to device design. Various design parameters such as the shape of the surfaces in contact with the person, size, mass characteristics, and the position and posture of each part are assumed to be relevant. Below, we describe the method of designing the motion trajectory pattern of the device.

An initial posture $\boldsymbol{x}_{init}$ and a final posture $\boldsymbol{x}_{goal}$ are decided in advance based on the posture simulation results. $\boldsymbol{x}$ is a vector containing the values of the design parameters. The initial trajectory $\mathbf{P}_0 = [\boldsymbol{x}_{01}\ \boldsymbol{x}_{02}\ ...\ \boldsymbol{x}_{0L}]$, which is the route that optimally minimizes the total physical burden, is obtained with Dijkstra method using the evaluation value E of discrete analysis results as the cost. After that, nonlinear optimization is performed using the following objective function to produce a smoother trajectory $\mathbf{P} = [\boldsymbol{x}_1\ \boldsymbol{x}_2\ ...\ \boldsymbol{x}_L]$.

$$\begin{aligned} \min : & \sum_{l=1}^{L-1} (w_{c1}C_1 + w_{c2}C_2 + w_{c3}C_3) \\ & C_1 = \|\boldsymbol{x}_{l+1} - \boldsymbol{x}_l\| \{max(E(\boldsymbol{a}, \boldsymbol{x}_{l+1}), E_{th}) - E_{th}\} \\ & C_2 = \|\boldsymbol{x}_{l+1} - \boldsymbol{x}_l\|^2 \\ & C_3 = \|\boldsymbol{x}_l - \boldsymbol{x}_{0l}\|^2 \\ \text{subject to} : & \mathbf{0} \le \boldsymbol{x}_l \le \mathbf{1} \quad (l = 1, ..., L) \\ & \boldsymbol{x}_1 = \boldsymbol{x}_{init},\ \boldsymbol{x}_L = \boldsymbol{x}_{goal} \end{aligned} \tag{8}$$

where w_{c1}, w_{c2}, and w_{c3} are weights. C_1 is the path integral of the evaluation value, and a reference value is available, the path avoids physical burden exceeding that value by setting it as a threshold E_{th}. C_2 evaluates the smoothness of the trajectory, and C_3 evaluates the closeness of the approximation to the initial path. This process allows us to design the trajectory in consideration of various design indicators including physical burden on the user.

III. Example of Device Design for Verification

A. Mockup of transfer support robot

We developed a mockup that imitates the structure of the robotic care device Hug for the verification experiment. The Hug has two degrees of freedom; the part supporting the user's chest can translate vertically and rotate in forward and backward. Figure 4 shows the developed mockup. Although this mockup does not include electrical actuators, the position and attitude of the plate supporting the upper body can be adjusted manually. This allows a static reproduction of the situation of standing assistance by delivered by the Hug

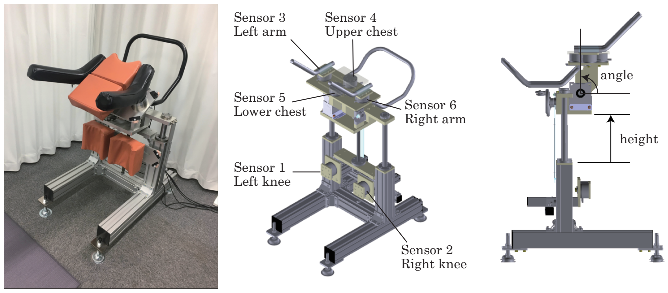

Fig. 4. Experimental mockup with force sensors for measuring contact forces.

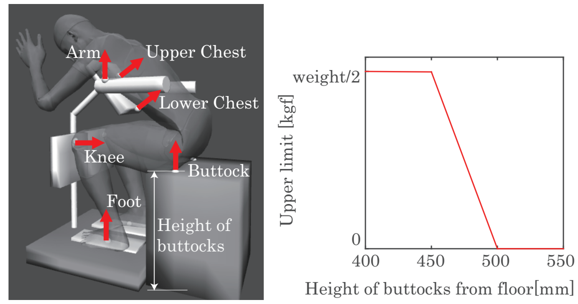

Fig. 6. Contact force vectors and upper limit of contact force on buttocks.

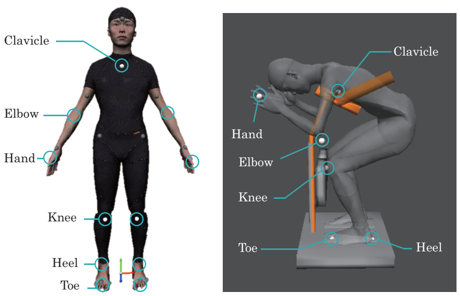

Fig. 5. Feature points on human and device for posture estimation.

device. In order to measure the reaction forces between human and the device, a total of six force and torque sensors are arranged at the left and right knee rests, the armrest, and the upper and lower parts of the chest cushion.

B. Modeling and physical burden analysis

In this section, we describe the analysis of the physical load on the user with the experimental assist mockup. The load–evaluation maps were generated based on the simulation results of the physical load when the user leans on the device. The joint torques and the contact forces are then analyzed with the method described in section II.

First, models of the mockup and the user were prepared and the postures of the user were estimated. The user is modeled assuming 167.5 cm height and 62 kg weight. This is roughly the average height of Japanese adults; and the weight is determined assuming a BMI of 22. In the posture estimation using inverse kinematics, we forced correspondence on the surface of the device and the body surface of the user as shown in Fig. 5 , and obtained the user's posture. The height of the device was varied from 0 to 210 mm in 35 mm increments and the forward inclination was varied from 0 to 55 deg in 5 deg increments.

Then, physical load analysis is performed for those postures. Figure 6 shows the contact force vectors that are assumed in the simulation. *Foot* is the reaction force from the floor, *Buttock* indicates the reaction forces from the chair, and the others are contact forces with the device, for a total of ten contact points. Since *Arm*, *Buttock*, *Knee*, and *Foot* are symmetrical, only the forces applied to left side is displayed in fig. 6. The contact force with the buttocks should be zero when the buttocks are detached from the chair. The height of the buttocks is then used to determine the upper limit of the contact forces. We confirmed experimentally that the force on the buttocks is at most about half of the user's body weight when sitting on a chair, limiting the sum of contact forces to half of the body weight even when the buttocks are at a relatively low position. These constraints are illustrated in Fig. 6. The weights in the Eq. (4) were empirically determined. It is preferable to set w_b greater than w_f and w_j because the smaller weight w_b increases the error with respect to the motion of the floating base [17]. In this simulation, we chose $w_b = 1$ and $w_f = w_j = 1 \times 10^{-2}$ so that the error in the force of the base link is suppressed to 0.03% or less of the body weight. The coefficient of friction is assumed to be 0.5 and the friction cone is approximated as ten ridgelines.

Figure 7 shows the simulation result of the contact force norm with respect to the device parameters. Since the results for the arms and legs are almost symmetrical, the results of only one side are shown in the figure. The following characteristics are notable.

- When both the height and the angle are small, the force received at the knee, the arms, and upper and lower chest are small, since the user is supposed to be sitting on the chair.
- When the height increases, the contact forces on the axilla (Fig. 7(a)) increase.
- When the angle becomes large, the chest cushion supports the weight of the upper body, so the load shifts from the arm (Fig. 7(a)) to the chest (Fig. 7(b),(c)).

These are natural results consistent with our experiences. As for joint torque analysis, the maximum values of the hip extension torque, the knee extension torque and the ankle plantar flexion torque are 6.62 Nm, 9.09 Nm, and 4.25 Nm respectively. Compared to the maximum voluntary torque of an average Japanese adult male [18], all the results are less than 10% different, as shown in Table I. Even considering that the torque required for normal sit-to-stand motion is about 50–100 Nm [19], we expect that the average adult male can maintain posture almost without using the lower limbs in this condition.

TABLE I

ESTIMATED JOINT TORQUE OF LOWER LIMBS.

	Maximum value in simulation [Nm]	Average maximum torque for males in their 20's [Nm] [18]	Expected exerted rate [%]
Hip extension	6.62	99.88	6.6
Knee extension	9.09	108.33	8.4
Plantar flexion	4.25	59.97	7.1

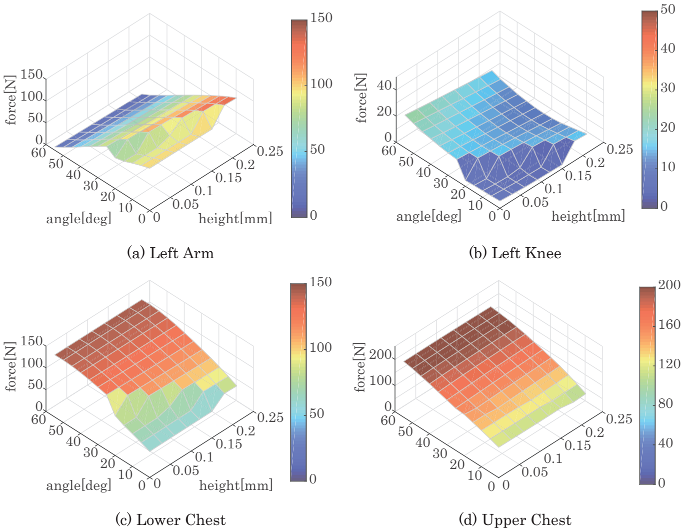

Fig. 7. Simulated contact forces between human and device / environment with respect to posture parameters (height, angle) of device. The values change greatly around the line connecting (angle = 25, height = 0) and (angle = 0, height = 0.2) because the buttocks lift off from the chair at this point.

C. Generation of sample trajectories

Based on the results in the previous section, the following four trajectories are generated from the evaluation map to verify the proposed design framework:

A) Minimizing contact forces acting on the axilla (Right Arm + Left Arm)
B) Maximizing contact forces acting on the axilla (Right Arm + Left Arm)
C) Minimizing contact forces acting on the chest (Upper Chest + Lower Chest)
D) Maximizing contact forces acting on the chest (Upper Chest + Lower Chest)

These conditions are selected because the device aims to reduce physical the burden by supporting the weight mainly through the chest and users tend to feel discomfort when the contact force to the axilla is strong. The device posture parameters of height and angle are normalized to the minimum and maximum values. Each evaluation factor is also normalized and approximated using the following fifth degree polynomial, and the coefficient vector $\boldsymbol{a}_k = \{a_{\alpha\beta}\}$

Fig. 8. Sites measured by EMG.

Fig. 9. Experimental scene.

is obtained using least–squares method.

$$\hat{E}_k\left(\boldsymbol{a}_k, \boldsymbol{x}\right) = \sum_{\alpha,\beta} a_{\alpha\beta}\left(x_1\right)^{\alpha}\left(x_2\right)^{\beta}$$
$$\left(\alpha, \beta \in \mathcal{Z},\ 0 \leq \alpha + \beta \leq 5,\ \alpha \geq 0,\ \beta \geq 0\right) \tag{9}$$

For maximization, the burden evaluation map is reversed and used in the same way as it is for minimization. The initial posture (seated posture) $\boldsymbol{x}_{init}$ is set as Height = 70 [mm], Angle = 0 [deg], and the final posture (standing posture) $\boldsymbol{x}_{goal}$ is set as Height = 150 [mm], Angle = 55 [deg]. The threshold E_{th} in the objective function Eq. (8) is set to $E\left(\boldsymbol{a}, \boldsymbol{x}_{init}\right)$, and represents the cost at the initial seated posture because the posture before standing up requires less effort from the user. The weights are set as $w_{c1} = w_{c2} = 1 \times 10^{-3}$, $w_{c3} = 1 \times 10^{-5}$. The generated trajectories are shown on the evaluation map in Figs. 10, 11. The state of the posture change of the user when passing through each trajectory is also shown in the figures. The validity of these trajectories was verified in the human subject experiments described in the next section.

IV. EXPERIMENTAL VERIFICATION

A subject experiment was performed to verify the feasibility of the proposed design method.

A. Method

1) Subjects: The subjects were five healthy adult males (aged 26 ± 2 years old, height 167.5 ± 2.8 cm, weight 64.9 ± 8.3 kg). All the subjects gave informed consent before participating. This study was approved by the research ethics committee of AIST(2016-677).

2) Data collection: In the experiments, the contact forces between the human and the mockup were measured using 6-axis force sensors (BFS series and PFS series, Leptrino Co., Ltd., See Fig. 4). The muscle activities were measured with surface electromyogram (EMG) sensors (Trigono, Delsys Inc.) at the vastus lateralis, biceps femoris, and gastrocnemius (See Fig. 8), which are related to hip extension, knee extension, and ankle plantar flexion. The sampling frequency was 1 kHz for both force and EMG sensors. Here, EMG is expressed in terms of the IEMG [%MVC] value normalized

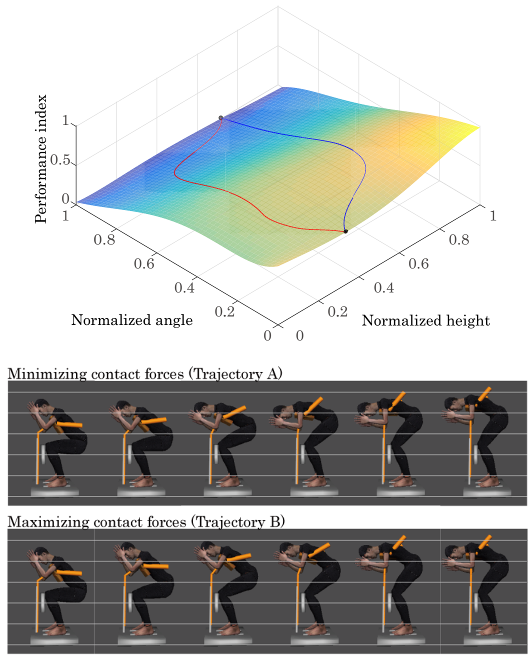

Fig. 10. Evaluation map of the contact force on the axilla and generated trajectories. The red line is trajectory A, which is intended to minimize the contact force, and the blue line is trajectory B, which is intended to maximize the contact force.

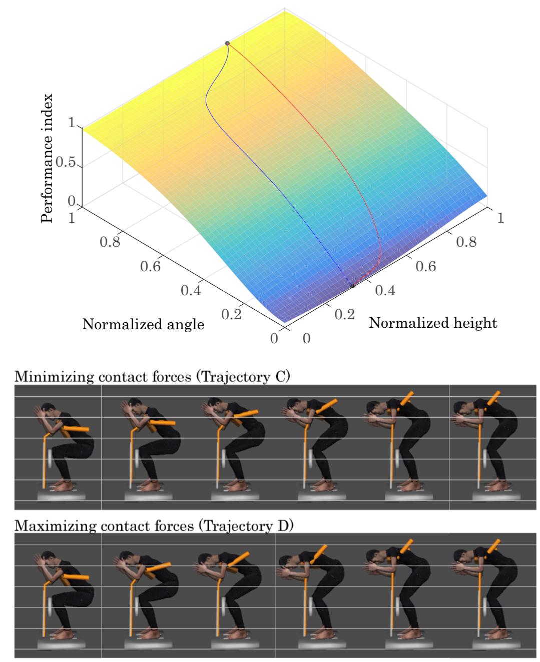

Fig. 11. Evaluation map of the contact force on the chest and generated trajectories. The red line is trajectory C, which is intended to minimize the contact force, and the blue line is trajectory D, which is intended to maximize the contact force.

to the maximum voluntary contraction (MVC) measured in advance, after applying a bandpass filter of 10–500 Hz and full-wave rectification.

3) Procedure: Sixteen postures were measured for the device, in combinations of changes in the height to 0, 70, 140, 210 [mm], and the angle to 0, 18, 37, 55 [deg]. Measurements were performed three times in each posture. The function of supporting the sit-to-stand motion was explained to the subjects in advance, and subjects were instructed to relax as much as possible. The subjects were also instructed not to grasp the device and not to lift their bodies with the power of the arms.

B. Results

1) Contact force: An example of the measured contact force is shown in Fig. 12. In the graph, first the mean value of three measurements is plotted on the 4 × 4 grid corresponding to different postures. A colored surface is then drawn by linear interpolation to visualize the overall distribution of contact force.

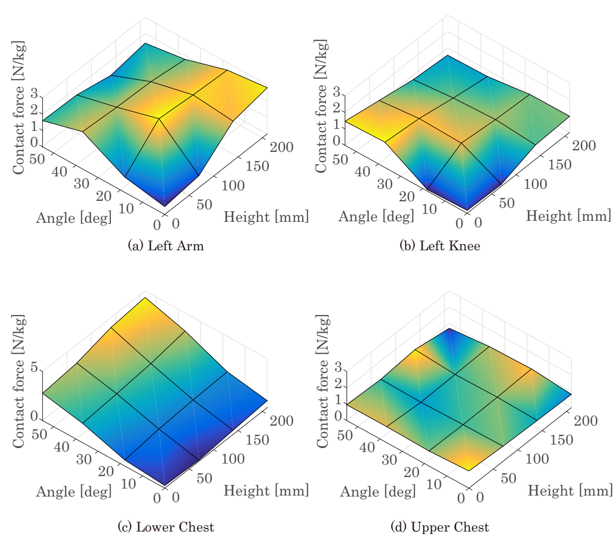

Fig. 12. Examples of measured contact forces. The contact force is divided by the body weight.

Figure 13 shows the sum of the *Left Arm* and *Right Arm* forces applied to the axilla, and the trajectories A and B are superimposed on it. Similarly, Fig. 14 shows trajectories C, D plotted on the sum of the forces *Upper Chest* and *Lower Chest* applied to the chest. The contact forces are divided by the body weight of each subject. The trajectories described in the section III-C are plotted on the surface to obtain the load evaluation values. As can be seen in the figures, both the contact forces have a graph shape similar to the simulation results indicated in Figs. 10, 11, except that the experimental values are smaller than the simulation value in the sitting posture (around 0.4 or less in the normalized height vs. 0.8 or less in the normalized height). If the multipoint contact condition changes greatly during motion, such as completely moving away from the chair like this device, the simulation may be improved by changing the weight setting of the load analysis according to the contact conditions.

To evaluate the physical burden of each trajectory, path integrals of the contact forces along the trajectories were calculated. Tables II and III show the calculation results. The calculated value for trajectory B is larger for all subjects than trajectory A, which was intended to minimize the forces to the axilla. Similarly, the burden in the trajectory D is larger than trajectory C, which was intended to minimize the forces to the chest. This confirms that the results were as expected.

2) Muscle activity: The EMG value was also checked for each trajectory. The simulations in section III-B showed that the device maintains posture mechanically with a small joint torque for adult men. However, if the subject is maintaining posture by the power of their muscles without relying on the device, the contact forces with device may decrease. Figure 15 shows the mean values of IEMG along trajectory, which are linearly interpolated like the contact forces were. For all subjects and trajectories, since IEMG is less than 8% MVC, we confirmed that the magnitudes of muscle activities were sufficiently small. Although the muscle activities were comparable in all trajectories, the target contact forces did decrease with the trajectories intended to minimize them. These results confirm that the proposed design method can generate a trajectory that places less burden on the selected body part.

V. Conclusion

In this paper, we proposed a simulation–based design protocol that optimizes device parameters of a robot that undergoes complex interaction with human based on an analysis using a digital human model. We also developed a mockup that imitates a robotic care device for supporting the sit–to–stand movement, and measured the contact forces and muscle activity when using the supportive device to verify the feasibility of the proposed design method. The result confirmed that the proposed protocol allows designers to improve the device for a specific goal such as reduction of the external forces on the selected body parts.

In this paper, the device model was divided into several parts, and the contact forces were represented by one resultant force for each part. It is one of the future tasks to analyze more detailed pressure distribution by considering the surface shapes and physical characteristics of the device and human. Furthermore, in the case of multi-point contact, the solution for the contact force / joint torque that satisfies a given mechanical condition is not unique. These values would depend on various factors such as the user's physical characteristics, the allowable value of contact force, the shapes of the device and the frictional force. Different types of robotic devices can be analyzed by the proposed method, but it may be necessary to change the weightings of optimization depending on the device and target user. In the simulations discussed above, the upper limit for the contact force to the buttocks was empirically determined. We consider that incorporating values that can be measured relatively easily in simulation conditions will also help in finding reasonable solutions. We plan to apply the proposed analysis to different types of devices, to test the framework's generality and to improve the versatility of the proposed method.

Acknowledgment

We would like to thank Ko Ayusawa for assistance with the simulations. We thank Fuji Machine Mfg. Co., Ltd. for information on the transfer support device *Hug*.
This research was partly supported by METI/AMED Robotic Devices for Nursing Care Project; and JSPS Grant-in-Aid for Scientific Research (A) 17H00768.

References

[1] World Health Organization, "World report on ageing and health", 2015.
[2] J. Smedley, P. Egger, C. Cooper, D. Coggon, "Manual handling activities and risk of low back pain in nurses. Occupational and environmental medicine". 52(3), 160–163, 1995.
[3] J.M. Burnfield, Y. Shu, et al., "Kinematic and electromyographic analyses of normal and device-assisted sit-to-stand transfers". Gait & posture. 36(3), 516–522, 2012.
[4] F. DallaLibera, Y. Tsusaka, et al., "Analysis of velocity's influence on forces and muscular activity in the context of sit-to-stand motion assisted by an elderly care robot". Proc. of 2016 IEEE/RSJ Int. Conf. on Intelligent Robots and Systems. 717–724, 2016.
[5] M. Ding, R. Ikeura, et al., "Comfort estimation during lift-up using nursing–care robot–RIBA". Proc. of First Int. Conf. on Innovative Engineering Systems. 225–230, 2012.
[6] P. M. Bush, S. Gaines, F. Gammoh, S. Wooden, "A comparison of software tools for occupational biomechanics and ergonomic research". Ergonomics - A Systems Approach. 65–118, 2012.
[7] P. Blanchonette, "Jack human modelling tool : A review". Technical report, Air Operations Division Defence Science and Technology Organisation, 2009.
[8] M. Damsgaard, J.Rasmussen, "Analysis of musculoskeletal systems in the AnyBody Modeling System". Simulation Modelling Practice and Theory. 14(8), 1100–1111, 2006.
[9] M. Geravand, P. Z. Korondi, et al., "Human sit-to-stand transfer modeling towards intuitive and biologically-inspired robot assistance". Autonomous Robots. 41(3), 575–592, 2017.
[10] Mobility support robot – Hug, FUJI CORPORATION, `https://www.fuji.co.jp/items/hug/hugt1`.
[11] Y. Endo, M. Tada, M. Mochimaru, "Dhaiba: development of virtual ergonomic assessment system with human models". Proc. of The 3rd Int. Digital Human Symposium, 2014.
[12] Y. Endo, M. Tada, M. Mochimaru, "Estimation of Arbitrary Human Models from Anthropometric Dimensions". Int. Conf. on Digital Human Modeling and Applications in Health, Safety, Ergonomics and Risk Management. 3–14, 2015.
[13] Y. Imamura, K. Ayusawa, Y. Endo, E. Yoshida, "Simulation–based Design for Robotic Care Device: Optimizing Trajectory of Transfer Support Robot". Proc. of the 15th IEEE Int. Conf. on Rehabilitation Robotics. 851–856, 2017.
[14] N. Magnenat-Thalmann, D. Thalmann, "Human body deformations using joint-dependent local operators and finite-element theory". No. VRLAB-ARTICLE-2007-050, 243–262, 1990.
[15] Y. Nakamura, K. Yamane, Y. Fujita, I. Suzuki, "Somatosensory computation for man-machine interface from motion-capture data and musculoskeletal human model". IEEE Transactions on Robotics. 21(1), 58–66, 2005.
[16] K. Harada, M. Kaneko, "A sufficient condition for manipulation of envelope family". IEEE Transactions on Robotics and Automation. 18(4), 597–607, 2002.
[17] K. Ayusawa, G. Venture, Y. Nakamura, "Identification of the inertial parameters of a humanoid robot using unactuated dynamics of the base link". Proc. of IEEE-RAS Int. Conf. on Humanoid Robots, 1–7, 2008.

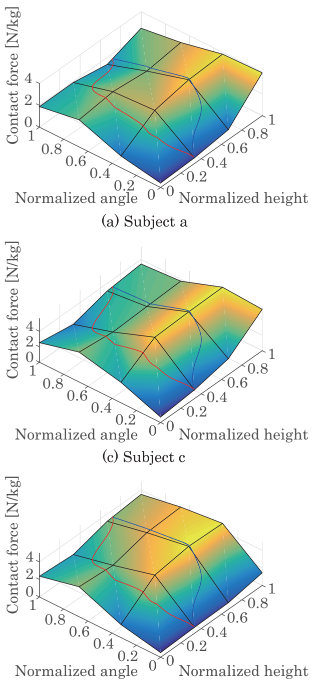

(a) Subject a (b) Subject b (c) Subject c (d) Subject d (e) Subject e

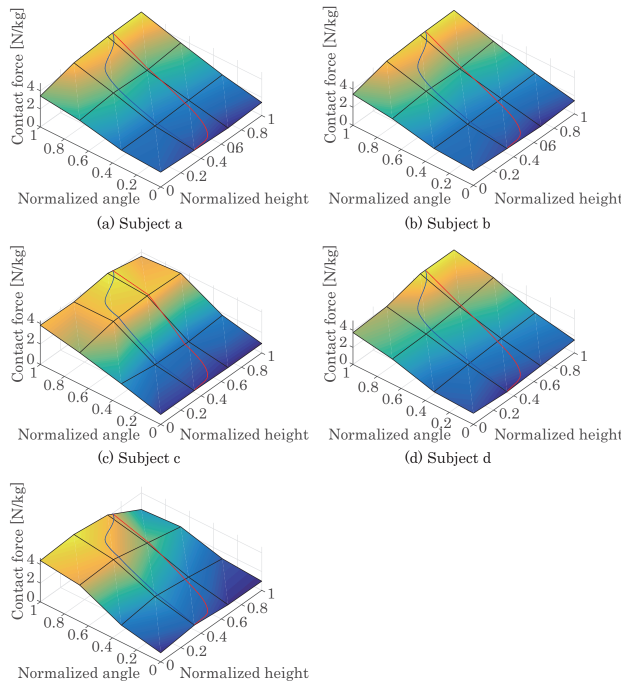

(a) Subject a (b) Subject b (c) Subject c (d) Subject d (e) Subject e

Fig. 13. Measured contact forces to axillas and trajectories designed based on simulation shown in Fig. 10 (Red line: trajectory A for minimizing contact force, Blue line: trajectory B for maximizing contact force).

Fig. 14. Measured contact forces to chest and trajectories designed based on simulation shown in Fig. 11 (Red line: trajectory C for minimizing contact force, Blue line: trajectory D for maximizing contact force).

TABLE II

PATH INTEGRAL OF CONTACT FORCES APPLIED TO THE ARMS ON THE TWO TRAJECTORIES SHOWN IN FIG. 13

Subject	Trajectory A [N/kg]	Trajectory B [N/kg]
a	2.10	2.79
b	3.65	4.42
c	3.23	4.34
d	3.33	4.26
e	2.78	4.12

TABLE III

PATH INTEGRAL OF CONTACT FORCES APPLIED TO THE CHEST ON THE TWO TRAJECTORIES SHOWN IN FIG. 14

Subject	Trajectory C [N/kg]	Trajectory D [N/kg]
a	2.79	3.52
b	1.97	2.80
c	2.68	3.39
d	2.91	3.46
e	2.57	3.74

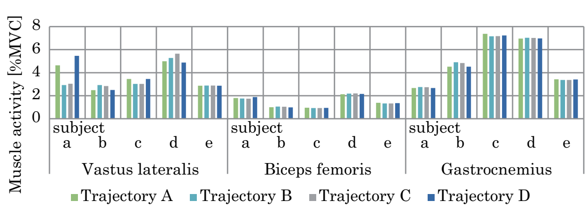

Fig. 15. Mean value of muscle activities on each trajectory.

[18] National Institute of Technology and Evaluation of JAPAN, "Data Book of human physical characteristics among healthy Japanese", `http://www.tech.nite.go.jp/human/jp/pdf/20FYdata/nite_humandatabook.pdf`, 2009.

[19] Y.C. Pai, M.W. Rogers, "Speed variation and resultant joint torques during sit-to-stand". Archives of physical medicine and rehabilitation. 72(11), 881–885, 1991.